Acta Pharmacologica Sinica

www.nature.com/aps

ARTICLE

The hybrid oncolytic peptide NTP-385 potently inhibits adherent cancer cells by targeting the nucleus

Hao Yin[1,2], Xi-tong Chen[3], Qiao-na Chi[4], Yan-nan Ma[3], Xing-yan Fu[3], Shan-shan Du[4], Yun-kun Qi[2,3] and Ke-wei Wang[1,2]

The use of oncolytic peptides with activity against a wide range of cancer entities as a new and promising cancer therapeutic strategy has drawn increasing attention. The oncolytic peptide LTX-315 derived from bovine lactoferricin (LfcinB) was found to be highly effective against suspension cancer cells, but not adherent cancer cells. In this study, we tactically fused LTX-315 with rhodamine B through a hybridization strategy to design and synthesize a series of nucleus-targeting hybrid peptides and evaluated their activity against adherent cancer cells. Thus, four hybrid peptides, NTP-212, NTP-217, NTP-223 and NTP-385, were synthesized. These hybrid peptides enhanced the anticancer activity of LTX-315 in a panel of adherent cancer cell lines by 2.4- to 37.5-fold. In model mice bearing B16-F10 melanoma xenografts, injection of NTP-385 (0.5 mg per mouse for 3 consecutive days) induced almost complete regression of melanoma, prolonged the median survival time and increased the overall survival. Notably, the administered dose of NTP-385 was only half the effective dose of LTX-315. We further revealed that unlike LTX-315, which targets the mitochondria, NTP-385 disrupted the nuclear membrane and accumulated in the nucleus, resulting in the transfer of a substantial amount of reactive oxygen species (ROS) from the cytoplasm to the nucleus through the fragmented nuclear membrane. This ultimately led to DNA double-strand break (DSB)-mediated intrinsic apoptosis. In conclusion, this study demonstrates that hybrid peptides obtained from the fusion of LTX-315 and rhodamine B enhance anti-adherent cancer cell activity by targeting the nucleus and triggering DNA DSB-mediated intrinsic apoptosis. This study also provides an advantageous reference for nucleus-targeting peptide modification.

Keywords: oncolytic peptides; LTX-315; rhodamine B; hybridization strategy; melanoma; ROS; DNA double-strand break; intrinsic apoptosis; nucleus-targeting peptides

Acta Pharmacologica Sinica (2023) 44:201–210; https://doi.org/10.1038/s41401-022-00939-x

INTRODUCTION

Cancer is rated as the main cause of death worldwide, and data from the International Agency for Research on Cancer suggests that globally, ~19.3 million people were diagnosed with cancer and that 10.0 million cancer patients died because of ineffective treatment in 2020 [1]. Chemotherapeutic drugs are conventional therapies to treat cancer and often experience losses in efficacy and potency due to drug resistance and toxicity [2, 3]. Therefore, it is necessary to identify novel effective anticancer agents with less toxicity. The host defense peptide lactoferricin (LfcinB) has been shown to have broad-spectrum antitumor activity [4], and based on its structure-activity relationship analysis, LTX-315 with more potent anticancer activity was designed [5–7]. LTX-315 provokes cancer cell death in two ways: the membranolytic effect [8] and the subsequent immune response [9, 10]. Unlike traditional peptides that block the PD-1/PD-L1 interaction [11, 12], LTX-315 induces immune responses in a cytosolic component-dependent manner [13, 14]. Specifically, this peptide causes rapid cell membrane lysis and subsequent leakage of the cytosolic components into the extracellular environment. Among cytosolic components, danger-associated molecular patterns (DAMPs) and high mobility group box protein 1 are able to induce specific immune reactions against cancer cells [15, 16]. LTX-315 inhibits xenograft growth in mice [17] and protects treated mice from the same sorts of tumor cells [18], demonstrating the generation of a specific immune response [10]. Although suspension cancer cells, such as lymphoma cells, are highly sensitive to LTX-315 [5], we found that most adherent cancer cells were resistant to this peptide with IC_{50} values >50 μM after 24 h, making it necessary to improve the anti-adherent cancer cell activity of LTX-315.

Hybridization of different bioactive compounds is one of the most promising methods to discover novel and effective drugs in the field of medicinal chemistry [19]. The hybrid molecule, also called a conjugate, is a synthetic compound composed of two or more bioactive molecular fragments linked by at least one covalent bond. The hybridization strategy originated in nature, and in most cases, the hybrid molecule has been shown to possess stronger activity than the parent compounds [20]. For example, vincristine, a natural heterogeneous dimer, comprises vinblastine and catharanthine. Neither of its monomers shows anticancer activity, but their hybrid molecule has potent

[1]Department of Pharmacology, School of Pharmacy, Qingdao University Medical College, Qingdao University, #1 Ningde Road, Qingdao 266073, China; [2]Institute of Innovative Drugs, Qingdao University, 38 Dengzhou Road, Qingdao 266021, China; [3]Department of Medicinal Chemistry, School of Pharmacy, Qingdao University Medical College, Qingdao University, #1 Ningde Road, Qingdao 266073, China and [4]College of Chemical Engineering, Qingdao University of Science and Technology, Qingdao 266042, China
Correspondence: Shan-shan Du (shanshandu@qust.edu.cn) or Yun-kun Qi (qiyunkun@qdu.edu.cn) or Ke-wei Wang (wangkw@qdu.edu.cn)

Received: 20 April 2022 Accepted: 6 June 2022
Published online: 6 July 2022

anti-leukemia effects [21]. Rhodamine B, which is famous for its redshifted fluorescence, is a classic fluorescent dye with positive charges [22]. Studies have demonstrated that the cationic region of LTX-315 is imperative for its interaction with the cancer cell membrane, which has negative charges [15]. Hence, to increase the number of positive charges, we designed a series of hybrid peptides by tactically fusing LTX-315 with rhodamine B through distinct linkers.

In this study, we designed and synthesized a series of rhodamine B-modified LTX-315 peptides (hybrid peptides), and their effects on adherent cancer cell viability were evaluated. Moreover, rhodamine B endows hybrid peptides with red fluorescence, and we utilized this property to accurately detect the localization of the hybrid peptide within cells. Furthermore, there have been reports that LTX-315 could generate reactive oxygen species (ROS) in melanoma cells [23], and ROS would inflict oxidative injury to DNA [24]. Therefore, the effects of hybrid peptides on the ROS levels, DNA damage, and intrinsic apoptosis were also investigated in adherent cancer cells.

MATERIALS AND METHODS

Synthesis of hybrid peptides

The hybrid peptides were prepared using 9-fluorenylmethoxycarbonyl (Fmoc)-based solid-phase peptide synthesis in a normal air-bath thermostatic oscillator [25]. In particular, DIC/Oxyma-based coupling reactions at 50 °C were applied to improve the synthetic efficiency [25–27]. Briefly, 160 mg of Rink Amide AM resin (0.05 mmol, 1 eq, Tianjin Nankai Hecheng Technology) was swelled in a DMF/DCM = 1:1 (*v*/*v*) solution for 1 h. The Fmoc group of the resin was removed by two treatments with 20% piperidine in DMF (5 min and 10 min) at 50 °C, followed by thorough washing with DMF and DCM. Subsequently, after the Fmoc-amino acid (4 eq, GL Biochem) was preactivated with DIC (8 eq, Titan Scientific) and Oxyma (4 eq, Titan Scientific) for 5 min at room temperature, the mixture was added to the resin. After 15 min of reaction at 50 °C, the resin was washed with DMF and DCM. The Kaiser test was conducted to monitor the completeness of amino acid coupling. A double coupling reaction was performed for 15–25 min if necessary.

After the coupling reaction, the resin was thoroughly washed with DMF and DCM. The Fmoc group was removed by two treatments with 20% piperidine in DMF at 50 °C (3 min and then 6 min). Subsequently, the resin was thoroughly washed, and then the next coupling procedure was conducted.

After coupling the amino acid residues and the linker, a mixed solution of rhodamine B (6 eq), HATU (2.8 eq), HOAt (3 eq), and DIPEA (6 eq) in DMF was added to the resin. The coupling of rhodamine B to the N-terminus was carried out three times (30 min, 40 min, and then 50 min) at 28 °C. After coupling rhodamine B, the peptide-bound resin was treated with the cleavage cocktail (TFA/phenol/water/thioanisole/EDT, 82.5:5:5:5:2.5, v/v/v/v/v) for 2.5–3.0 h at room temperature. After completion of the cleavage reaction, the TFA solution was concentrated with pure argon. The crude peptides were obtained by precipitation with cold Et_2O followed by centrifugation (three times). Then, the crude peptide was dissolved in H_2O/CH_3CN and purified by semipreparative RP-HPLC (Shimadzu). After lyophilization, the solid target peptides were obtained with a purity above 96%.

Fluorescence spectroscopy

NTP-385 was dissolved in tri-distilled water before recording the spectra using a FlexStation 3 multimode microplate reader (Molecular Devices, San Francisco, USA). The excitation and emission spectra of NTP-385 (100 μM, 300 μL/well) were acquired in 96-well black microplates. Different concentrations of NTP-385 (300 μL/well) were used to obtain the relationship between concentration and fluorescence intensity.

Cell culture

Human cervical cancer cells (HeLa, National Infrastructure of Cell Line Resource (NICR)), human liver cancer cells (Huh-7, NICR), human lung cancer cells (A549, NICR), and murine melanoma cells (B16-F10, National Collection of Authenticated Cell Culture) were cultured in Dulbecco's modified Eagle's medium (DMEM; Gibco) with 10% fetal bovine serum (FBS; PAN-Biotech). Human liver cancer cells ($HepG_2$ and Hep3B, NICR) and human cervical cancer cells (C-33A, NICR) were cultured in minimum essential medium (MEM; Gibco) supplemented with 10% FBS. Human ovarian cancer cells (ES-2 and SK-OV-3, NICR) were cultured in McCoy's 5 A medium (Boster) with 10% FBS. The human cervical cancer cell line Ca Ski (NICR) was cultured in RPMI-1640 medium (Gibco) with 10% FBS. All cells were cultured at 37 °C in 5% CO_2.

MTT assay

To evaluate the anticancer activities of the hybrid peptides, an MTT assay was conducted on adherent cancer cells. Peptides were dissolved in DMSO to generate 30 mM stock solutions. Cancer cells were seeded at a density of 15,000–20,000 cells/well in 96-well plates and incubated with 0, 3.125, 6.25, 12.5, 25, 50, or 100 μM oncolytic peptides for 24 h. Then, 15 μL of MTT (5 mg/mL, Aladdin) was added to each well before incubation for 4 h at 37 °C. The culture medium was removed from the wells, and 150 μL of DMSO was added to each well for 60 min. Then, the optical density (*OD*) was measured at 490 nm using a microplate reader (Tecon). The inhibition rate (%) was calculated as (OD_{control}-$OD_{\text{experimental}}$)/(OD_{control}-OD_{blank})*100%. The half-maximal inhibitory concentration (IC_{50}) of each peptide was calculated by IBM SPSS Statistics 22 software from three independent experiments.

Antitumor efficacy in vivo

Tumor xenografts were established by subcutaneous transplantation of 10^5 B16-F10 cells into the right flanks of 6-week-old CB6F1 mice (Charles River, male). The animals were housed under pathogen-free conditions. The research protocol was in accordance with the institutional guidelines of the Animal Care and Use Committee. Using the calipers for measurements, tumor volumes were defined as 0.5*(length*width^2). Once the xenografts in the transplanted mice were larger than 100 mm^3, the mice were randomized into three groups. The control group ($n = 7$) was injected intralesionally with 50 μL of normal saline only for 3 days. The two experimental groups were administered 50 μL of LTX-315 (10 mg/mL, only half of the usual LTX-315 dose) ($n = 10$) or NTP-385 ($n = 10$) intralesionally for 3 days. Injection solutions were prepared by dissolving the peptides in normal saline before the experiments. Animals were euthanized when the maximum diameter of the xenograft exceeded 2 cm or the tumor presented ulcerations, after which the tumor was resected and weighed.

Immunohistochemistry

Mice carrying B16-F10 xenografts were intralesionally administered normal saline, 0.5 mg of LTX-315 (50 μL*10 mg/mL) or 0.5 mg of NTP-385 for 3 continuous days. Injection solutions were prepared by dissolving the peptides in normal saline before the experiments. One day later, the mice were sacrificed, and the tumors were carefully harvested and fixed in 4% PFA. Immunohistochemical examinations were analyzed as previously described [28]. Briefly, samples were embedded in paraffin and cut into 6 μm thick slices. Slices were dewaxed and rehydrated and then underwent heat-induced epitope retrieval before immunostaining. To avoid interference from endogenous peroxidase, the sections were pretreated using 3% H_2O_2 for 25 min. After blocking with BSA, the sections were incubated with anti-CD8 (1:400, GB13429, Servicebio), anti-Ki67 (1:500, GB111141, Servicebio), or anti-CD31 (1:100, GB13063, Servicebio) antibodies overnight at 4 °C, followed by several washes and incubation with secondary antibodies (1:200, GB23303 or

GB23204, Servicebio). DAB (Servicebio) was used as a substrate, and hematoxylin was used as a counterstain. Subsequently, images were acquired using a microscope and analyzed by Image-Pro Plus 6.0 software.

Cancer cell uptake and fluorescence imaging assay
$HepG_2$ cells were cultured in 24-well plates and allowed to adhere overnight. Thereafter, the medium was removed and replaced with 500 μL of MEM without phenol red containing 10 μg/mL Hoechst 33258 (Invitrogen) and 200 nM MitoTracker Green (Beyotime). After 30 min of incubation, the medium was discarded again, and the cells were incubated separately with DMSO, 50 μM NTP-385, 50 μM NTP-221 or 50 μM LTX-315 plus 50 μM rhodamine B for different lengths of time. Following three washes, the cells were observed under a fluorescence microscope (Nikon). Because NTP-221 emits blue fluorescence, the mitochondria were labeled with MitoTracker Red (Beyotime), and the nuclei were labeled with SYBR Green I (Solarbio). Manders' colocalization (MC) coefficients obtained from ImageJ were used to evaluate the degree of colocalization.

Membranolytic activity assay
Propidium iodide (PI) was utilized to evaluate the cell membrane integrity, as it interacts with the DNA from the cells whose membranes were destroyed and emits red fluorescence. $HepG_2$ cells were seeded in 24-well plates overnight for incubation. Cells were stained with Hoechst 33258 for 30 min, after which the medium was discarded and replaced with 500 μL of phenol red-free MEM containing 2 μg/mL PI (Aladdin) plus DMSO, 25 μM NTP-385, or 25 μM LTX-315 for different lengths of time as indicated. Then, the supernatants were discarded, and the cells were washed three times before immediate observation by fluorescence microscopy (Nikon).

Western blot assay
Immunoblotting was conducted as described previously [29]. $HepG_2$ cells treated with NTP-385 for 12 h were lysed with RIPA lysis buffer (Solarbio) containing phosphatase inhibitor cocktail I (C0002, TargetMol, USA) and protease inhibitor cocktail (C0001, TargetMol, USA). A BCA Protein Assay Reagent Kit (Thermo Fisher) was used to determine the protein concentration. Total proteins were separated by 12% SDS–PAGE and electrotransferred to polyvinylidene fluoride membranes (Millipore). The membranes were blocked with QuickBlock™ Blocking Buffer for Western Blot (Beyotime) and then incubated with primary antibodies against GAPDH (1:10,000, ab181602, Abcam), cleaved caspase-9 (1:1000, 9505, CST), cleaved caspase-3 (1:1000, 9661, CST), γ-H2AX (1:1000, 9718, CST), Bax (1:5000, 50599, Proteintech) and Bcl-2 (1:1000, 12789, Proteintech) and a secondary antibody. The proteins in the blots were visualized with an ECL Western blotting detection system (Bio-Rad). Image Lab software (Bio-Rad) was used for protein quantification.

ROS measurement
Cellular ROS levels were detected with the ROS Assay Kit (Beyotime) using the fluorescent probe DCFH-DA. DCFH-DA is not fluorescent, and after entering the cell, it is hydrolyzed by intracellular esterase to produce nonfluorescent DCFH. The ROS in the cell can oxidize DCFH to produce fluorescent DCF, and the fluorescence intensity of DCF reflects the ROS level. $HepG_2$ cells cultured in six-well plates were harvested using trypsin-EDTA (Thermo Fisher) and incubated with NTP-385 at a series of concentrations for 2 h. Subsequently, the cells were stained with 10 μM DCFH-DA. After 20 min, the treated cells were washed three times with MEM without phenol red and transferred to 96-well black microplates in triplicate. All fluorescent intensities were measured with FlexStation (excitation at 488 nm and emission at 525 nm). To visualize the distribution of ROS in cells, cells treated with 25 μM NTP-385 for different lengths of time were stained with 10 μM DCFH-DA and observed by fluorescence microscopy (Nikon).

Cell apoptosis assay
Cell apoptosis was analyzed using Hoechst 33258 and GreenNuc™ caspase-3 assay kits (a green fluorescent dye that indicates apoptotic cells, Beyotime). Adherent cancer cells seeded in 24-well plates were incubated with the indicated agents for 12 h, after which the cells were washed with PBS and stained with the caspase-3 assay kit and Hoechst 33258. The simultaneous use of these two dyes allows normal and apoptotic cells to be distinguished by fluorescence microscopy.

RESULTS

Synthesis and characterization of the hybrid peptides
Four hybrid peptides, NTP-212, NTP-217, NTP-223, and NTP-385, were synthesized by conjugating rhodamine B to LTX-315 (Fig. 1a, Extended Data Fig. 1). The analytical RP-HPLC chromatograms and ESI-MS spectra confirmed the purities and molecular weights of the synthetic peptides (Extended Data Fig. 2). Oncolytic peptides with positive charges made the solution basic, and under this condition, rhodamine B was nonfluorescent [30], so the red fluorescence from the hybrid peptides was extremely weak (Fig. 1b, c). The fluorescence assay showed that NTP-385 had maximum excitation at 560 nm and maximum emission at 590 nm (Fig. 1b), displaying a bathochromic shift compared to rhodamine B (excitation: 554 nm and emission: 578 nm). NTP-385 exhibited the most intense fluorescence among the four hybrid peptides at the same concentration (Extended Data Fig. 3), so NTP-385 was used to carry out further mechanistic research.

Inhibition of adherent cancer cell proliferation by hybrid peptides
LTX-315, intermediates or hybrid peptides (3.125, 6.25, 12.5, 25, 50, and 100 μM) were used to treat 10 adherent cancer cell lines for 24 h. The hybrid peptides inhibited the proliferation of a series of adherent cancer cell lines in a dose-dependent manner and enhanced the anticancer activity of LTX-315 by ~2.4- to 37.5-fold in the different cell lines (Fig. 2a, Table 1). Interestingly, we found a super oncolytic peptide-resistant cell line, Hep3B, whose viability showed little change even after treatment with 100 μM LTX-315 for 24 h (Fig. 2a, Table 1, Extended Data Fig. 4), but the hybrid peptides still had potent anticancer activity toward this cell line (Fig. 2a, Table 1, Extended Data Fig. 4).

The activities of the hybrid peptides with different linkers were basically the same (Fig. 2a, Table 1), indicating that the type of linker is not important for activity. Next, to determine whether covalent linkage is necessary for hybrid peptide activity, we examined the effect of LTX-315 plus rhodamine B on cell viability. The results showed that regardless of the mixed proportions of LTX-315 and rhodamine B, their combination did not significantly improve activity (Fig. 2b, Extended Data Table 1), demonstrating that covalent linkage plays an important role in hybrid peptide activity. Subsequently, to validate the importance of the two parent compounds, rhodamine B-modified aurein 1.2 (a non-cationic oncolytic peptide, NTP-242) and another fluorophore, coumarin-modified LTX-315 (NTP-221), were synthesized (Extended Data Fig. 2). We found that there was no significant difference between the activities of the two modified peptides and those of the corresponding parent peptides (Fig. 2c, Extended Data Table 2). Overall, the combination of rhodamine B and LTX-315 and covalent linkage between these two parts are vital for the improvement in anticancer activity, and none of these components is dispensable.

The time–response curve illustrated that the hybrid peptides needed 24 h to exert their maximum effects (Fig. 2d), which demonstrated that the rapid necrosis reported by previous research [5] was not the full mechanism of action. Compared

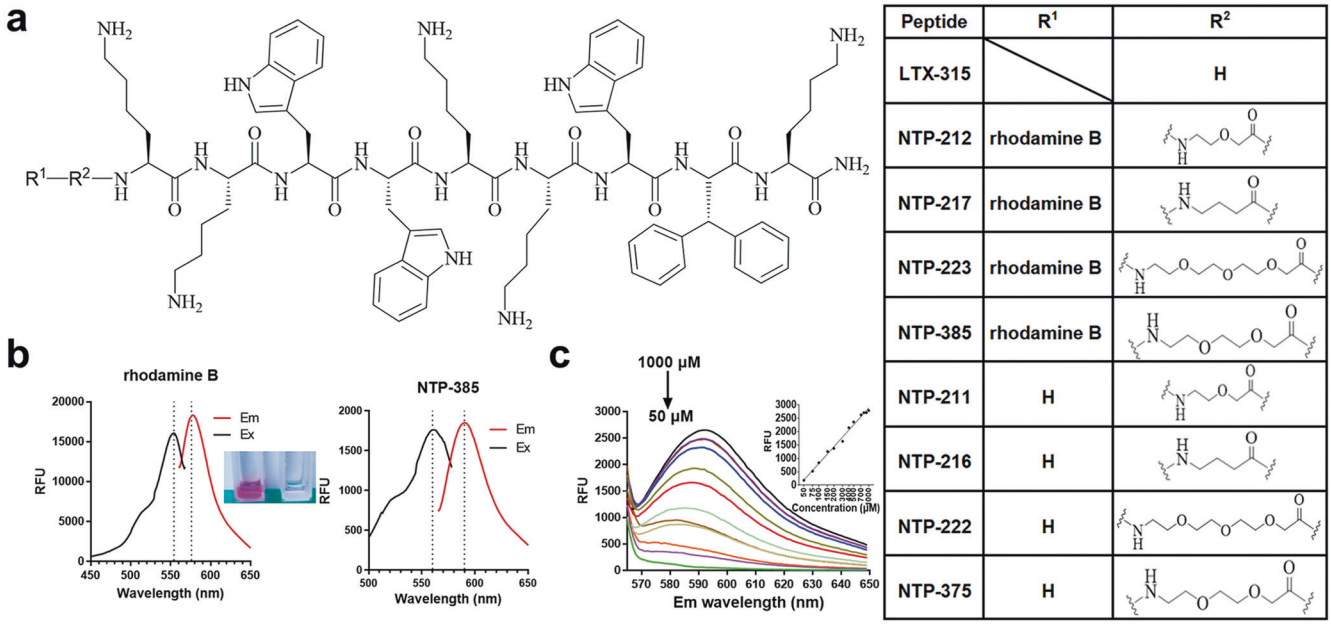

Peptide	R^1	R^2
LTX-315		H
NTP-212	rhodamine B	
NTP-217	rhodamine B	
NTP-223	rhodamine B	
NTP-385	rhodamine B	
NTP-211	H	
NTP-216	H	
NTP-222	H	
NTP-375	H	

Fig. 1 Structures and fluorescence spectroscopic properties. a Structures of LTX-315, the intermediates, and the hybrid peptides. **b** Fluorescence spectra of 30 μM rhodamine B (left) and 100 μM NTP-385 (right) in tri-distilled water. Insets, photographs of 30 μM rhodamine B (left) and 100 μM NTP-385 (right) in tri-distilled water. **c** Fluorescence intensities of NTP-385 at various concentrations.

with LTX-315 activity peaking at 12 h, the hybrid peptides peaked at 24 h and remained active for 72 h, which may be because hybridization not only increased activity but also improved peptide stability.

Inhibition of melanoma growth by NTP-385 in mice

We assessed the in vivo tumoricidal efficacy of the hybrid peptides in CB6F1 mice bearing B16-F10 xenografts (Fig. 3a). Among the four hybrid peptides tested in vitro (Table 1), NTP-385 was the most potent inhibitor of B16-F10 cancer cells and was subsequently chosen to test its in vivo tumoricidal efficacy. Compared with the control group, the administration of 0.5 mg of NTP-385 per mouse for 3 consecutive days resulted in notable tumor growth inhibition (~86.2% by tumor weight), prolonged median survival time, and increased overall survival (Fig. 3b–e). At the end of this experiment (28 days), complete cancer remission was observed in the majority of mice treated with NTP-385 (overall survival = 80%) and in nearly half of the mice treated with LTX-315 (median survival time = 26.5 days; overall survival = 50%) (Fig. 3d, e). In contrast, cancer growth in the control group mice was uninhibited, and all animals were sacrificed within 9 days (median survival time = 8 days). Interestingly, LTX-315 at half of the usual dose did not lead to necrotic skin injury or scabbing (data not shown), but the anticancer activity of LTX-315 dropped, while that of NTP-385 remained significant.

Within the injected area, we found a dramatic accumulation of $CD8^+$ T cells in the NTP-385-treated mice (Fig. 3f, g), which significantly permeated from the injected area to the noninjected area, suggesting that the hybrid peptide promoted antineoplastic immunity. In addition, CD31 is expressed primarily in endothelial cells and can be used to determine the degree of cancer angiogenesis in histological tissue sections. The IHC assay revealed a decreased level of CD31 in the NTP-385-treated group compared to the control group (Fig. 3f, g), suggesting that angiogenesis and the rapid tumor growth were inhibited. Ki67 is a nuclear protein that is normally considered a marker for cell proliferation. A marked reduction in the expression of Ki67 was observed in the tumors of mice treated with NTP-385 (Fig. 3f, g), demonstrating that NTP-385 inhibited cancer cell proliferation in xenografts.

Induction of cell membranolysis by NTP-385

Based on a previous study showing that LTX-315 can cause loss of cell membrane integrity [15], we postulated that the hybrid peptides could also exert a membranolytic effect to permeate into cells. To test this hypothesis, we carried out time-lapse fluorescence imaging of PI, a fluorescent probe that only penetrates damaged cell membranes to intercalate into DNA and emit red fluorescence. As depicted in Fig. 4a and Extended Data Fig. 5, it took only 15 min for 25 μM NTP-385 to alter the plasma membrane integrity of the slim majority of cells (~40%). Cells incubated for 45 min with the hybrid peptide showed a great deal of PI incorporation into the nuclei (>80%) (Fig. 4b), which was compatible with quick membranolysis. Regarding the speed and extent of the membranolytic effect, there was no significant difference between NTP-385 and LTX-315 treatment (Fig. 4a, b). LTX-315 (25 μM) was sufficient to devastate the plasma membrane, but the MTT assay suggested that 25 μM was ineffective (Fig. 2a), which may be because adherent cells are resistant to membranolysis to a certain extent. Furthermore, the anticancer activity of the hybrid peptides involves other mechanisms besides membranolysis.

Accumulation of NTP-385 in the cell nuclei

To interpret the different action patterns of hybrid peptides and LTX-315, live-cell imaging was performed using DMSO, NTP-385, LTX-315 plus rhodamine B, or coumarin-modified LTX-315 (NTP-221). First, the MTT assay validated that NTP-221 did not change the anticancer activity of LTX-315 (IC_{50}: 103.9 μM for NTP-221 versus 109.8 μM for LTX-315) (Fig. 2c). NTP-221 rapidly penetrated the cell membrane and accumulated in the mitochondria without being detected in the cell nucleus (Fig. 4c, d), which echoes a previous study [23]. However, NTP-385 had only a short stay in the cytoplasm and finally accumulated in the cell nuclei (Fig. 4c, d), which subverts the previously suggested mechanism underlying LTX-315.

Elevation of the ROS level and the induction of DNA double-strand break (DSB) by NTP-385

As previous research indicated that LTX-315 increased the ROS level in melanoma cells [23], we measured ROS levels before and

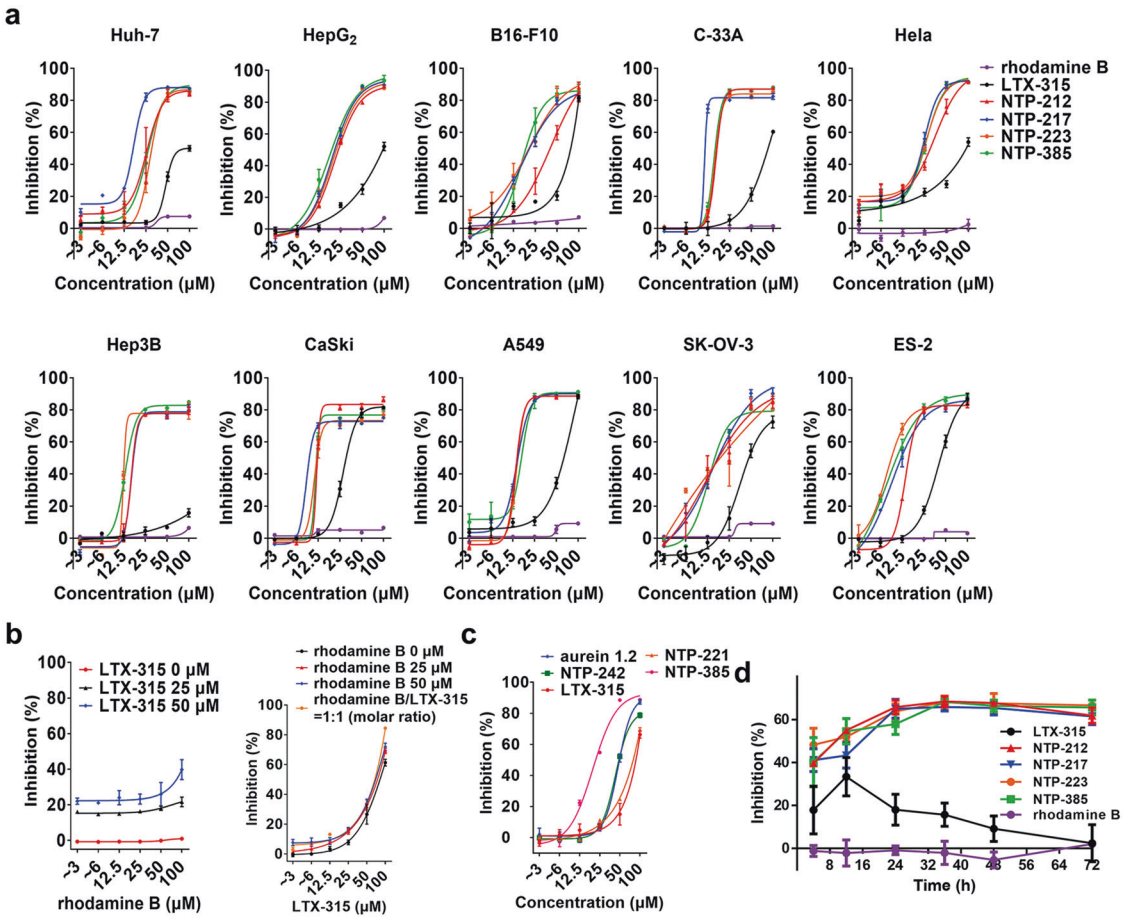

Fig. 2 Anticancer activity of oncolytic peptides against adherent cancer cells. a Adherent cancer cells were incubated with oncolytic peptides for 24 h and then subjected to the MTT assay. **b** $HepG_2$ cells were exposed to a series of concentrations of rhodamine B in the presence of LTX-315 (left panel) or a series of concentrations of LTX-315 in the presence of rhodamine B (right panel) for 24 h and then subjected to the MTT assay. **c** $HepG_2$ cells were exposed to LTX-315, NTP-221 (coumarin-modified LTX-315), aurein 1.2 (a noncationic oncolytic peptide), NTP-242 (rhodamine B-modified aurein 1.2), or NTP-385 for 24 h and then subjected to the MTT assay. **d** $HepG_2$ cells were exposed to 25 μM oncolytic peptides for the indicated lengths of time and then subjected to the MTT assay. Error bars indicate the SD, and the results are representative of three independent experiments.

Table 1. Activity against adherent cancer cell lines as determined by MTT assay (IC_{50} ± SEM in μM, 24 h).

Peptide	HeLa	$HepG_2$	B16-F10	C-33A	Huh-7	Hep3B	CaSki	A549	SK-OV-3	ES-2
LTX-315	127.8 ± 13.4	109.8 ± 16.0	104.3 ± 28.5	100.5 ± 18.7	139.5 ± 34.8	>500	35.7 ± 1.3	54.7 ± 0.7	58.2 ± 2.3	58.3 ± 16.0
NTP-212	25.2 ± 4.3	38.9 ± 1.1	44.0 ± 2.8	18.3 ± 0.8	29.3 ± 1.4	23.0 ± 4.0	10.8 ± 1.6	18.8 ± 4.2	21.2 ± 0.9	15.4 ± 2.2
NTP-217	20.2 ± 2.0	23.0 ± 3.6	24.6 ± 0.2	13.5 ± 0.1	16.8 ± 1.1	23.5 ± 2.9	7.3 ± 0.9	18.8 ± 4.2	18.2 ± 0.6	8.9 ± 3.1
NTP-223	19.3 ± 1.9	22.0 ± 3.0	27.4 ± 4.8	19.7 ± 3.4	35.9 ± 2.1	13.3 ± 0.8	11.5 ± 0.4	19.5 ± 1.9	15.8 ± 1.8	6.4 ± 1.0
NTP-385	20.9 ± 1.6	21.0 ± 3.0	23.4 ± 5.9	19.0 ± 1.0	30.5 ± 2.5	13.3 ± 1.5	11.5 ± 0.1	18.5 ± 1.9	14.8 ± 1.8	7.4 ± 1.0
NTP-211	98.0 ± 17.7	126.7 ± 23.2	80.1 ± 9.2	87.1 ± 5.0	166.6 ± 131.9	>500	35.5 ± 2.1	50.7 ± 1.1	44.5 ± 1.2	33.6 ± 5.5
NTP-216	91.3 ± 16.1	86.9 ± 9.9	96.8 ± 1.3	75.3 ± 3.9	96.1 ± 2.5	>500	32.5 ± 2.6	36.6 ± 4.7	36.7 ± 4.3	41.5 ± 3.0
NTP-222	135.9 ± 22.1	159.0 ± 29.5	108.8 ± 4.4	70.4 ± 2.1	91.7 ± 4.9	>500	35.7 ± 0.5	35.7 ± 0.5	44.7 ± 8.5	50.1 ± 13.4
NTP-375	161.5 ± 29.3	96.1 ± 0.8	93.1 ± 2.1	71.1 ± 6.1	121.0 ± 20.9	>500	41.0 ± 0.6	41.0 ± 0.6	45.1 ± 4.1	34.4 ± 4.8

Data from three independent experiments are presented as the mean ± SEM.

after treatment with NTP-385. NTP-385 dose-dependently increased the ROS levels in $HepG_2$ cells (Fig. 5a), and at the same concentration, the ROS-generating ability of NTP-385 was more potent than that of LTX-315 (Fig. 5b).

We further investigated the localization of DCFH-DA-derived fluorescence in $HepG_2$ cells by fluorescence microscopy. Initially, intense green fluorescence was detected in the cytoplasm after treatment with 25 μM NTP-385, and over time, this fluorescence transferred gradually from the cytoplasm into the nucleus (Fig. 5c, Extended Data Fig. 6). Eventually, the cell nuclei showed the most intense green fluorescence accompanied by diminished cytoplasmic fluorescence (Fig. 5d), which echoes the distribution of the hybrid peptides within cells. These results showed that membrane-impermeable DCFH derived from DCFH-DA could enter the

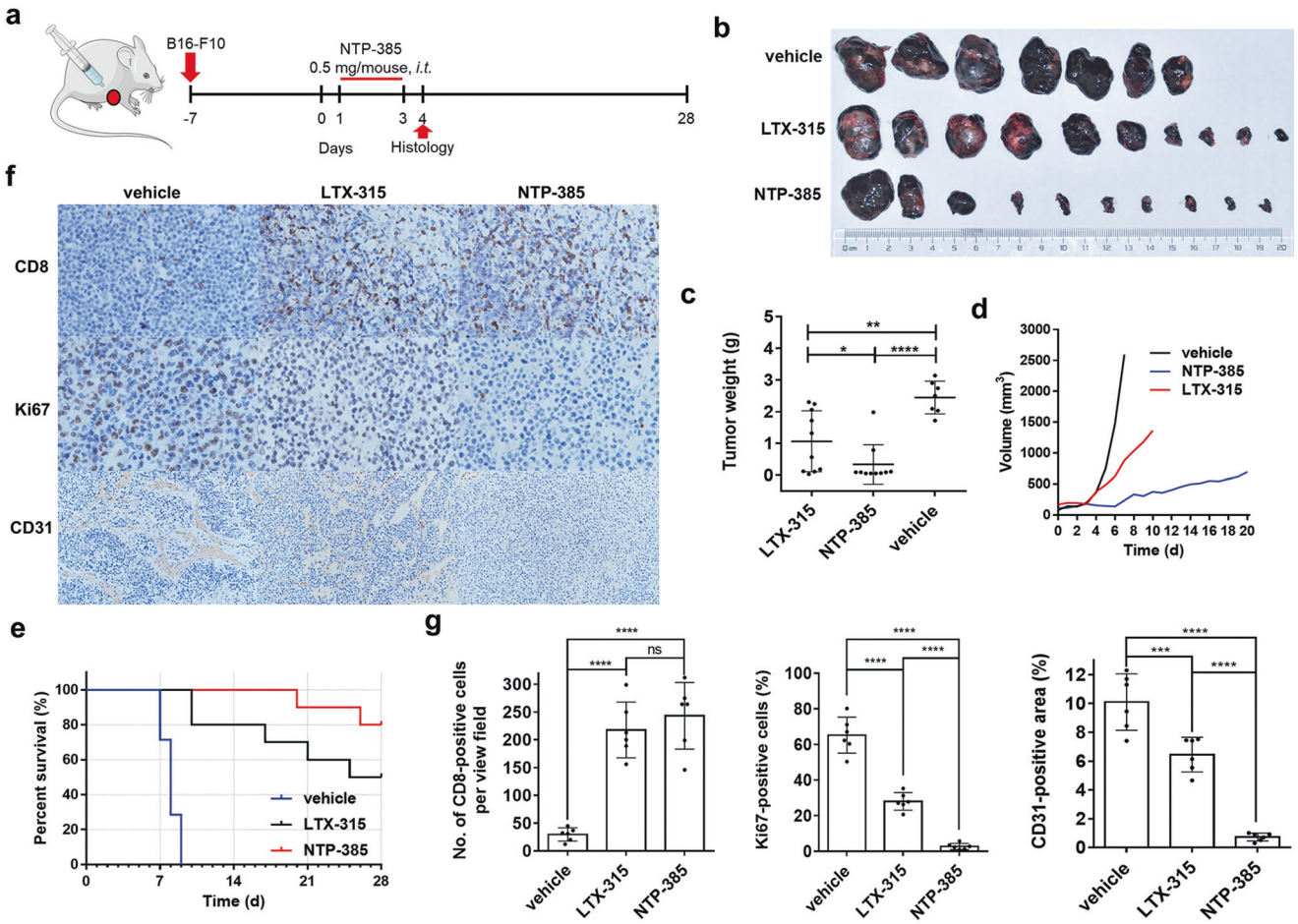

Fig. 3 Hybrid peptides inhibited tumor growth. a Schematic illustration of the timeline for the therapeutic experiments. **b** Images of the excised B16-F10 tumors. **c** Weights of the B16-F10 tumors. **d** Tumor growth kinetics of the different groups. **e** Survival analysis of the B16-F10 tumor-bearing mice. **f** Immunohistochemistry for CD8, Ki67, and CD31 in B16-F10 melanoma sections (10× for CD8 and Ki67 and 4× for CD31). **g** Quantification of CD8, Ki67, and CD31 expression in melanoma sections. $n = 6$, mean ± SD. All P values were determined by multiple comparisons after one-way ANOVA. $^{*}P < 0.05$, $^{**}P < 0.01$, $^{***}P < 0.001$, $^{****}P < 0.0001$; ns not significant.

nucleus and rapidly accumulate ROS from the cytoplasm into the nucleus. Therefore, it is plausible to suppose that the hybrid peptides destroyed the nuclear membrane, allowing substances within the cytoplasm to have free access to the nucleus.

ROS are especially prone to inflict oxidative damage on DNA, so we also examined the level of the DNA DSB marker γ-H2AX. Exposure of $HepG_2$ cells to NTP-385 resulted in a dose-dependent increase in the expression of γ-H2AX (Fig. 5e). Moreover, in the MTT assay, adding the antioxidant *N*-acetyl-*L*-cysteine (NAC) significantly reduced the cytotoxicity induced by NTP-385 in $HepG_2$ cells (Fig. 5b, f). NAC also ameliorated NTP-385-induced DNA DSB, which indicated that this DNA damage effect was dependent on ROS (Fig. 5g). By comparison, a relatively small DNA damage effect was observed in cells treated with LTX-315 (Fig. 5g), which may be because LTX-315 could not disrupt the nuclear membrane and produce enough ROS.

Induction of intrinsic apoptosis in adherent cancer cells by NTP-385

Unrepairable DNA DSB induces apoptosis [31], so apoptosis-related experiments were performed. The caspase-3/7 activity assay showed that the levels of active caspase-3/7 increased in a concentration-dependent manner in $HepG_2$ cells treated with different concentrations of NTP-385 for 12 h (Fig. 6a, b). In comparison with LTX-315 at 25 μM, which increased the caspase-3/7 activity by only 3.03%, NTP-385 at 12.5 μM resulted in a significant increase in active caspase-3/7 by 40.6% (Fig. 6b). In contrast, preincubation with the pan-caspase inhibitor z-VAD-fmk (20 μM) caused a significant rightward shift in the NTP-385-mediated concentration-dependent cytotoxicity (Fig. 6c), which further confirmed the generation of active caspase in $HepG_2$ cells after treatment with NTP-385. Western blot analysis showed that the expression levels of Bax together with cleaved caspase-3 and cleaved caspase-9 dose-dependently increased in response to different concentrations of NTP-385 (Fig. 6d), whereas that of Bcl-2 decreased in the presence of different concentrations of NTP-385 (Fig. 6d, e). These results demonstrate that intrinsic apoptosis was induced by NTP-385 in adherent cancer cells.

DISCUSSION

In this study, by applying a hybridization strategy, we fused LTX-315 and rhodamine B through distinct linkers to obtain a series of nucleus-targeting hybrid peptides with potent cytotoxicity against adherent cancer cells. Adherent cancer cells are resistant to LTX-315 ($IC_{50} > 50$ μM for 24 h), but applying this strategy increased its activity against adherent tumor cells by approximately 2.4- to 37.5-fold in comparison with the LTX-315 prototype. Moreover, the therapeutic potential of the representative hybrid peptide NTP-385 was determined in a well-established murine B16-F10 melanoma model. At a dose of 0.5 mg per mouse (usual dose of LTX-315: 1 mg per mouse), LTX-315 did not lead to skin necrosis

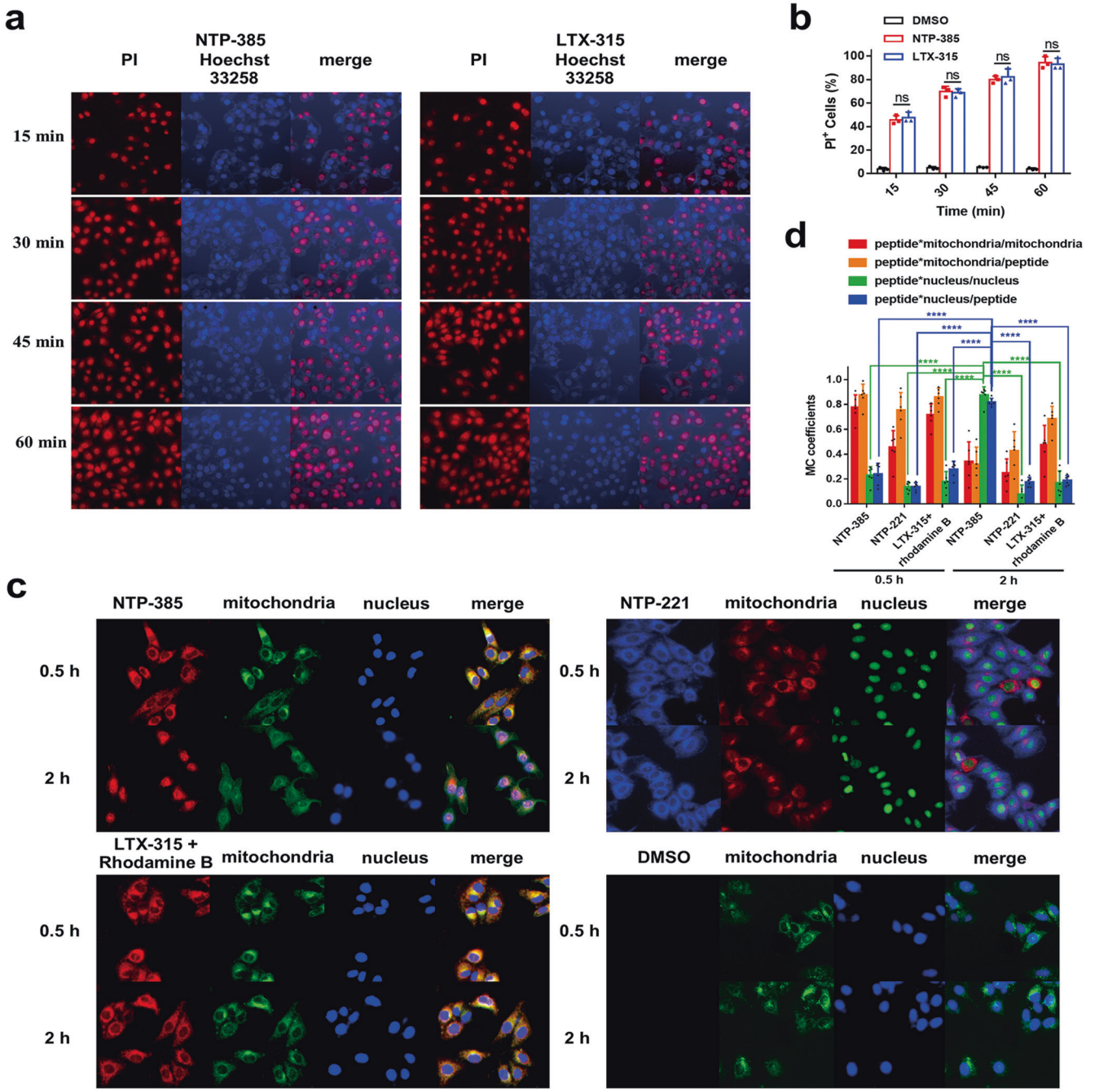

Fig. 4 Hybrid peptides caused membranolysis and accumulated in the nucleus of $HepG_2$ cells. a $HepG_2$ cells treated with 25 μM NTP-385 or LTX-315 were labeled with PI (10×). **b** Quantification of PI-positive cells. $n = 3$, mean ± SD. **c** Fluorescence images of $HepG_2$ cells treated with 50 μM NTP-385, 50 μM NTP-221, 50 μM LTX-315 plus 50 μM rhodamine B or DMSO (20×). **d** Manders' colocalization (MC) coefficients were obtained by ImageJ. MC coefficients are proportional to the fluorescence intensity of the colocalizing pixels or voxels in each color channel. One-way ANOVA, multiple comparisons. ****$P < 0.0001$; ns: not significant.

but showed relatively weak anticancer activity. In contrast, at a dose of 0.5 mg, NTP-385 exhibited satisfactory tumoricidal activity, and complete tumor regression was obtained in an overwhelming majority of the treated mice. However, the xenograft tumor model in this study uses homogeneous cells that lack tumor heterogeneity and unique tumor cell interactions, which may have limitations for drug efficacy evaluation [32]. Hence, the anticancer activity of hybrid peptides may need to be further tested in different tumor models, such as patient-derived xenografts, transgenic tumor models and heterogeneous tumor models [33]. In addition to intralesional injection, different delivery routes of hybrid peptides are also worth exploring.

LTX-315 fights against cancer cells by membranolysis and induced tumor-specific immune response [9]. In terms of membranolysis, PI staining analysis suggested that there was no significant difference in the speed or degree of membranolysis between LTX-315 and the hybrid peptides. This observation was similar for the induced immune response, where the CD8 immunohistochemical assay demonstrated that the percentage of $CD8^+$ T cells in the injection area after treatment with NTP-385

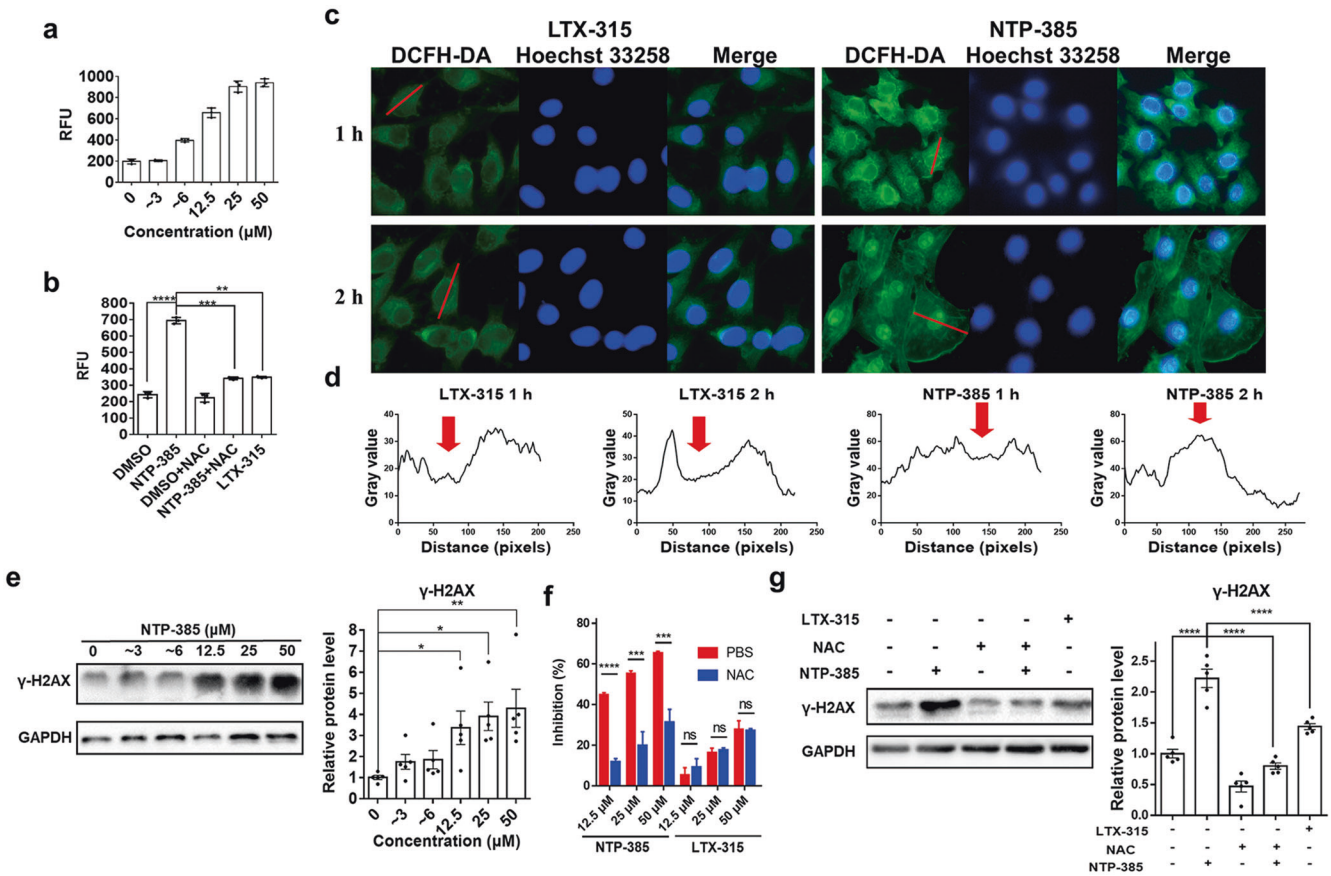

Fig. 5 Hybrid peptides induced ROS accumulation in the nucleus and DNA DSB in $HepG_2$ cells. a ROS levels were detected in $HepG_2$ cells treated with a series of concentrations of NTP-385 for 2 h using fluorometric analysis. $n = 3$, mean ± SD. **b** ROS levels were detected in $HepG_2$ cells treated with DMSO, 25 μM NTP-385, DMSO plus 10 mM *N*-acetyl-*L*-cysteine (NAC; antioxidant), 25 μM NTP-385 plus 10 mM NAC, or 25 μM LTX-315 for 2 h. $n = 3$, mean ± SD. **c** Fluorescence images of the ROS in $HepG_2$ cells were obtained at different times after treatment with 25 μM NTP-385 using DCFH-DA (20×). **d** Fluorescence intensities of the cell cross-sections (red line shown in **c**). The arrow indicates the cell nucleus. **e** γ-H2AX expression was measured using Western blot analysis (left panel) in $HepG_2$ cells treated with NTP-385 for 12 h. The right panel represents the quantification of γ-H2AX expression. $n = 5$, mean ± SEM. **f** $HepG_2$ cells were treated with NTP-385 alone or in combination with 10 mM NAC for 24 h and then subjected to the MTT assay. Blue: NAC treatment groups, Red: vehicle treatment groups. Error bars indicate the SD, and the results are representative of three independent experiments. *t*-test. **g** The expression of γ-H2AX in $HepG_2$ cells treated with DMSO, 25 μM NTP-385, DMSO plus 10 mM *N*-acetyl-*L*-cysteine (NAC), 25 μM NTP-385 plus 10 mM NAC, or 25 μM LTX-315 for 12 h and the quantification of γ-H2AX. $n = 5$, mean ± SEM. Unless otherwise indicated, all *P* values were determined by multiple comparisons after one-way ANOVA. $^*P < 0.05$, $^{**}P < 0.01$, $^{***}P < 0.001$, $^{****}P < 0.0001$.

was equal to that of LTX-315. Therefore, what leads to the increase in activity?

First, the high number of positive charges on LTX-315 enables it to bind in a nonspecific manner to the abundant negatively charged phospholipids on the surface of cancer cells, indicating that a positive charge plays an important role in cytotoxicity toward cancer cells [15]. The introduction of the cationic fluorophore rhodamine B increased the net positive charge on the peptides to augment the interaction between the hybrid peptide and the cancer cell plasma membrane.

Second, unlike LTX-315, which targets the mitochondria [23], the current data demonstrated that the hybrid peptides finally accumulated in the cell nucleus. In search of the distinct modes of action of the hybrid peptides and LTX-315, non-rhodamine B fluorophore-modified LTX-315 was synthesized. There was no significant difference in anticancer activity between the coumarin-modified LTX-315 (NTP-221) and LTX-315, demonstrating that the coumarin group did not affect the mode of action of LTX-315. Interestingly, by observing the distribution of the hybrid peptides in the cells, we obtained unexpected findings. The cell imaging assay suggested that NTP-221 accumulated in only the mitochondria and could not be detected in the cell nuclei, which is in accordance with previous research [23]. Nonetheless, the hybrid peptides eventually accumulated in the nucleus, which is very different from the parent peptide LTX-315. Correspondingly, after treatment with the hybrid peptides, a large amount of ROS was detected in the nucleus, and a relatively small amount was detected in the cytoplasm, whereas in the LTX-315 group, ROS was found in the cytoplasm and not in the nucleus. We presume that because hybrid peptides destroy the nuclear membrane, the ROS in the cytoplasm can readily enter the cell nucleus. However, why and how the hybrid peptides destroy the nuclear membrane need further study.

Third, ROS within the nucleus induced DNA DSB and intrinsic apoptosis. ROS can cause oxidative damage to DNA [34], which is in line with the result that after NTP-385 treatment, the level of γ-H2AX increased dramatically. Moreover, what exactly happens after the loss of nuclear membrane integrity is an interesting question that deserves to be investigated. Unrepairable DNA DSB triggers intrinsic apoptosis [35] via a pathway that has been well established. DNA DSB events can activate the tumor suppressor p53, resulting in the upregulation of some pro-apoptotic proteins, such as Bax, leading to the initiation of intrinsic apoptosis [31]. When severe loss of cell membrane integrity occurs, digestion by trypsin is fatal for cells. Additionally, Annexin-V can cross the

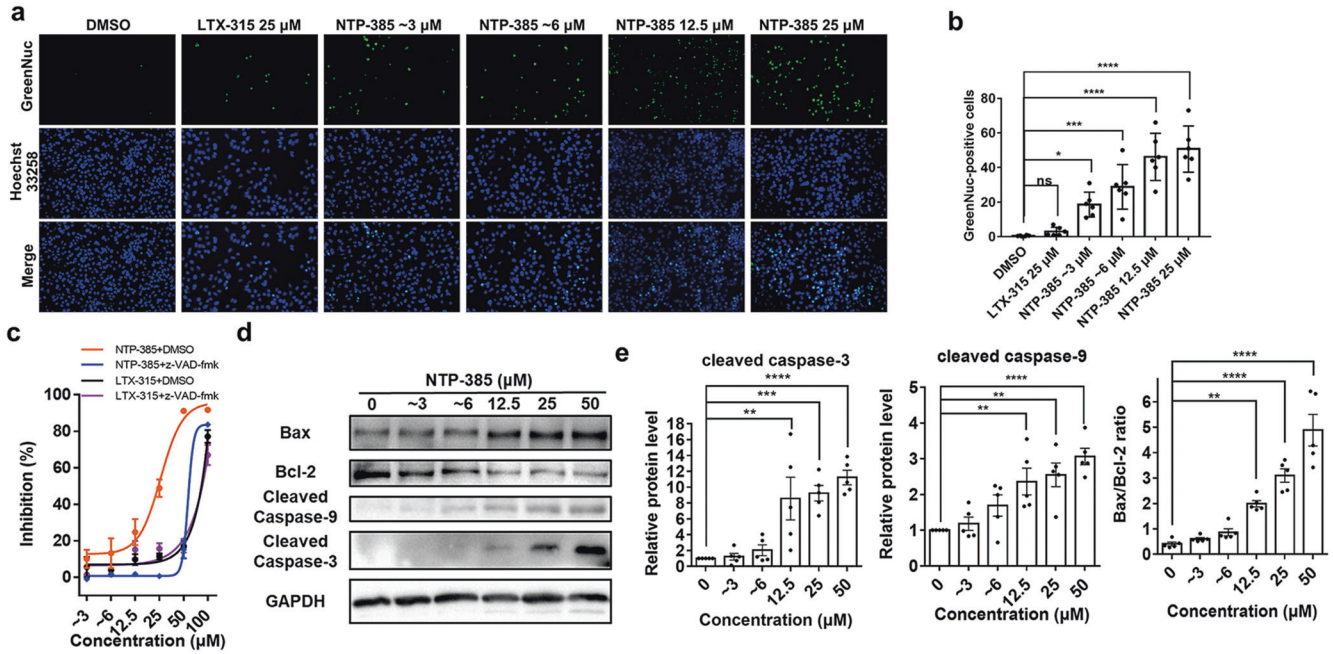

Fig. 6 Hybrid peptides induced intrinsic apoptosis in $HepG_2$ cells. a $HepG_2$ cells were treated with DMSO, LTX-315, or NTP-385 for 12 h. Cells were stained with a caspase-3/7 assay kit and Hoechst 33258 (4×). **b** The percentage of apoptotic cells was quantified by counting the ratio of active caspase-3-positive and Hoechst 33258-positive cells. **c** $HepG_2$ cells were treated with NTP-385 alone or in combination with 20 μM z-VAD-fmk for 24 h and then subjected to the MTT assay. **d** Bax, Bcl-2, cleaved caspase-9, and cleaved caspase-3 expression was measured using Western blot analysis in $HepG_2$ cells treated with NTP-385 for 12 h. **e** Quantification of Bax, Bcl-2, cleaved caspase-9, and cleaved caspase-3. The columns represent the mean ± SEM, $n = 5$. All P values were determined by multiple comparisons after one-way ANOVA. $^{*}P < 0.05$, $^{**}P < 0.01$, $^{***}P < 0.001$, $^{****}P < 0.0001$; ns: not significant.

fragmented membrane to bind with phosphatidylserine, bypassing the apoptotic state, so we did not carry out flow cytometry experiments but instead performed caspase-3/7 activity assays. The ability of these hybrid peptides to induce intrinsic apoptosis is supported by the below evidence. (i) In the intrinsic apoptosis pathway, the hybrid peptides downregulated the antiapoptotic protein Bcl-2 and upregulated the pro-apoptotic protein Bax. (ii) The hybrid peptides activated caspase-3 and −9. (iii) The pan-caspase inhibitor z-VAD-fmk reversed the cytotoxic effects of the hybrid peptides. It has been reported that the cytotoxicity of LTX-315 is not dependent on caspase activation [6] but NTP-385 is, which may be because NTP-385 can destroy the nuclear membrane and cause ROS to accumulate in the nucleus.

In conclusion, we found that nucleus-targeting hybrid peptides obtained from the fusion of rhodamine B and LTX-315 possess potent anti-adherent cancer cell activity. In addition to maintaining the membranolysis and tumor-specific immune response induction activities of LTX-315, the hybrid peptides also have their own special actions, including targeting the nucleus as well as induction of DNA DSB and intrinsic apoptosis. Hybrid peptides give rise to the loss of nuclear membrane integrity, which contributes to the rapid accumulation of ROS in the nucleus. Large amounts of ROS cause DNA DSB and further activate the intrinsic apoptotic pathway, resulting in the death of cancer cells. This study provides a reference for modifying peptides to target the nucleus, and our creative idea utilizing the hybridization strategy might become a potential method to speed up the development of oncolytic peptides.

ACKNOWLEDGEMENTS

This project was supported by grants from the National Natural Science Foundation of China (81973299, 22177058, 82003647), the China Postdoctoral Science Foundation (2020T130332, 2019M652307), and the Qingdao postdoctoral application research project.

AUTHOR CONTRIBUTIONS

HY designed research; HY performed research; YKQ designed oncolytic peptides; XTC, YNM and XYF synthesized peptides; HY and QNC performed MTT assay; HY and YKQ analyzed data; HY wrote the paper; SSD, YKQ and KWW prepared the paper.

ADDITIONAL INFORMATION

Supplementary information The online version contains supplementary material available at https://doi.org/10.1038/s41401-022-00939-x.

Competing interests: The authors declare no competing interests.

REFERENCES

1. Sung H, Ferlay J, Siegel RL, Laversanne M, Soerjomataram I, Jemal A, et al. Global Cancer Statistics 2020: GLOBOCAN Estimates of Incidence and Mortality Worldwide for 36 Cancers in 185 Countries. CA Cancer J Clin. 2021;71:209–49.
2. Zhitomirsky B, Assaraf YG. Lysosomes as mediators of drug resistance in cancer. Drug Resist Updat. 2016;24:23–33.
3. Wang N, Xie G, Liu C, Cong W, He S, Li Y, et al. Design, synthesis, and antitumor activities study of stapled A4K14-citropin 1.1 peptides. Front Chem. 2020;8:616147.
4. Mader JS, Richardson A, Salsman J, Top D, de Antueno R, Duncan R, et al. Bovine lactoferricin causes apoptosis in Jurkat T-leukemia cells by sequential permeabilization of the cell membrane and targeting of mitochondria. Exp Cell Res. 2007;313:2634–50.
5. Sveinbjornsson B, Camilio KA, Haug BE, Rekdal Ø. LTX-315: a first-in-class oncolytic peptide that reprograms the tumor microenvironment. Future Med Chem. 2017;9:1339–44.
6. Forveille S, Zhou H, Sauvat A, Bezu L, Muller K, Liu P, et al. The oncolytic peptide LTX-315 triggers necrotic cell death. Cell Cycle. 2015;14:3506–12.
7. Spicer J, Marabelle A, Baurain JF, Jebsen NL, Jossang DE, Awada A, et al. Safety, antitumor activity, and T-cell responses in a dose-ranging phase I trial of the oncolytic peptide LTX-315 in patients with solid tumors. Clin Cancer Res. 2021;27:2755–63.
8. Haug BE, Camilio KA, Eliassen LT, Stensen W, Svendsen JS, Berg K, et al. Discovery of a 9-mer cationic peptide (LTX-315) as a potential first in class oncolytic peptide. J Med Chem. 2016;59:2918–27.

9. Tornesello AL, Borrelli A, Buonaguro L, Buonaguro FM, Tornesello ML. Antimicrobial peptides as anticancer agents: functional properties and biological activities. Molecules. 2020;25:2850.
10. Nestvold J, Wang MY, Camilio KA, Zinocker S, Tjelle TE, Lindberg A, et al. Oncolytic peptide LTX-315 induces an immune-mediated abscopal effect in a rat sarcoma model. Oncoimmunology. 2017;6:e1338236.
11. Zhou X, Zuo C, Li W, Shi W, Zhou X, Wang H, et al. A novel D-peptide identified by mirror-image phage display blocks TIGIT/PVR for cancer immunotherapy. Angew Chem Int Ed. 2020;59:15114–8.
12. Chang HN, Liu BY, Qi YK, Zhou Y, Chen YP, Pan KM, et al. Blocking of the PD-1/PD-L1 interaction by a D-peptide antagonist for cancer immunotherapy. Angew Chem Int Ed. 2015;54:11760–4.
13. Eksteen JJ, Ausbacher D, Simon-Santamaria J, Stiberg T, Cavalcanti-Jacobsen C, Wushur I, et al. Iterative design and in vivo evaluation of an oncolytic antilymphoma peptide. J Med Chem. 2017;60:146–56.
14. Zhou H, Forveille S, Sauvat A, Yamazaki T, Senovilla L, Ma Y, et al. The oncolytic peptide LTX-315 triggers immunogenic cell death. Cell Death Dis. 2016;7:e2134.
15. Vitale I, Yamazaki T, Wennerberg E, Sveinbjørnsson B, Rekdal Ø, Demaria S, et al. Targeting cancer heterogeneity with immune responses driven by oncolytic peptides. Trends Cancer. 2021;7:557–72.
16. Luan X, Wu Y, Shen YW, Zhang H, Zhou YD, Chen HZ, et al. Cytotoxic and antitumor peptides as novel chemotherapeutics. Nat Prod Rep. 2021;38:7–17.
17. Wu Y, Lu D, Jiang Y, Jin J, Liu S, Chen L, et al. Stapled Wasp venom-derived oncolytic peptides with side chains induce rapid membrane lysis and prolonged immune responses in melanoma. J Med Chem. 2021;64:5802–15.
18. Liao HW, Garris C, Pfirschke C, Rickelt S, Arlauckas S, Siwicki M, et al. LTX-315 sequentially promotes lymphocyte-independent and lymphocyte-dependent antitumor effects. Cell Stress. 2019;3:348–60.
19. Meunier B. Hybrid molecules with a dual mode of action: Dream or reality? Acc Chem Res. 2008;41:69–77.
20. Mehta G, Singh V. Hybrid systems through natural product leads: an approach towards new molecular entities. Chem Soc Rev. 2002;31:324–34.
21. Tsogoeva SB. Recent progress in the development of synthetic hybrids of natural or unnatural bioactive compounds for medicinal chemistry. Mini-Rev Med Chem. 2010;10:773–93.
22. Mottram LF, Forbes S, Ackley BD, Peterson BR. Hydrophobic analogues of rhodamine B and rhodamine 101: potent fluorescent probes of mitochondria in living *C. elegans*. Beilstein J Org Chem. 2012;8:2156–65.
23. Eike LM, Yang N, Rekdal Ø, Sveinbjørnsson B. The oncolytic peptide LTX-315 induces cell death and DAMP release by mitochondria distortion in human melanoma cells. Oncotarget. 2015;6:34910–23.
24. Kawanishi S, Hiraku Y, Pinlaor S, Ma N. Oxidative and nitrative DNA damage in animals and patients with inflammatory diseases in relation to inflammation-related carcinogenesis. Biol Chem. 2006;387:365–72.
25. Chen XT, Wang JY, Ma YN, Dong LY, Jia SX, Yin H, et al. DIC/Oxyma-based accelerated synthesis and oxidative folding studies of centipede toxin RhTx. J Pep Sci. 2022;28:e3368.
26. Yin H, Chen X, Fu X, Ma Y, Xu Y, Zhang T, et al. Efficient chemical synthesis and oxidative folding studies of scorpion toxin peptide WaTx. Acta Chim Sin. 2022;80:444–52.
27. Ma Y, Liu Y, Wang J, Chen X, Yin H, Chi Q, et al. DIC/Oxyma based efficient synthesis and activity evaluation of spider peptide toxin GsMTx4. Chin J Org Chem. 2022;42:498–506.
28. Liu Z, Zhang S, Hou F, Zhang C, Gao J, Wang KW. Inhibition of Ca^{2+}-activated chloride channel ANO1 suppresses ovarian cancer through inactivating PI3K/Akt signaling. Int J Cancer. 2019;144:2215–26.
29. Yao X, Zhao CR, Yin H, Wang KW, Gao JJ. Synergistic antitumor activity of sorafenib and artesunate in hepatocellular carcinoma cells. Acta Pharmacol Sin. 2020;41:1609–20.
30. Birtalan E, Rudat B, Kolmel DK, Fritz D, Vollrath SBL, Schepers U, et al. Investigating rhodamine B-labeled peptoids: scopes and limitations of its applications. Biopolymers. 2011;96:694–701.
31. Roos WP, Kaina B. DNA damage-induced cell death by apoptosis. Trends Mol Med. 2006;12:440–50.
32. Liu T, Yao R, Pang Y, Sun W. Review on biofabrication and applications of heterogeneous tumor models. J Tissue Eng Regen Med. 2019;13:2101–20.
33. Teicher BA. Tumor models for efficacy determination. Mol Cancer Ther. 2006;5:2435–43.
34. Trachootham D, Alexandre J, Huang P. Targeting cancer cells by ROS-mediated mechanisms: a radical therapeutic approach? Nat Rev Drug Discov. 2009;8:579–91.
35. Bonner WM, Redon CE, Dickey JS, Nakamura AJ, Sedelnikova OA, Solier S, et al. γH2AX and cancer. Nat Rev Cancer. 2008;8:957–67.